

1N-26  
068191  
32p.



# **Corrosion Studies of 2195 Al-Li Alloy and 2219 Al Alloy With Differing Surface Treatments**

*M.D. Danford and M.J. Mendrek*

*Marshall Space Flight Center, Marshall Space Flight Center, Alabama*

## The NASA STI Program Office...in Profile

Since its founding, NASA has been dedicated to the advancement of aeronautics and space science. The NASA Scientific and Technical Information (STI) Program Office plays a key part in helping NASA maintain this important role.

The NASA STI Program Office is operated by Langley Research Center, the lead center for NASA's scientific and technical information. The NASA STI Program Office provides access to the NASA STI Database, the largest collection of aeronautical and space science STI in the world. The Program Office is also NASA's institutional mechanism for disseminating the results of its research and development activities. These results are published by NASA in the NASA STI Report Series, which includes the following report types:

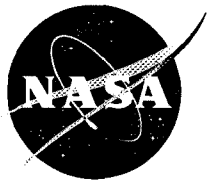
- **TECHNICAL PUBLICATION.** Reports of completed research or a major significant phase of research that present the results of NASA programs and include extensive data or theoretical analysis. Includes compilations of significant scientific and technical data and information deemed to be of continuing reference value. NASA's counterpart of peer-reviewed formal professional papers but has less stringent limitations on manuscript length and extent of graphic presentations.
- **TECHNICAL MEMORANDUM.** Scientific and technical findings that are preliminary or of specialized interest, e.g., quick release reports, working papers, and bibliographies that contain minimal annotation. Does not contain extensive analysis.
- **CONTRACTOR REPORT.** Scientific and technical findings by NASA-sponsored contractors and grantees.

- **CONFERENCE PUBLICATION.** Collected papers from scientific and technical conferences, symposia, seminars, or other meetings sponsored or cosponsored by NASA.
- **SPECIAL PUBLICATION.** Scientific, technical, or historical information from NASA programs, projects, and mission, often concerned with subjects having substantial public interest.
- **TECHNICAL TRANSLATION.** English-language translations of foreign scientific and technical material pertinent to NASA's mission.

Specialized services that complement the STI Program Office's diverse offerings include creating custom thesauri, building customized databases, organizing and publishing research results...even providing videos.

For more information about the NASA STI Program Office, see the following:

- Access the NASA STI Program Home Page at <http://www.sti.nasa.gov>
- E-mail your question via the Internet to [help@sti.nasa.gov](mailto:help@sti.nasa.gov)
- Fax your question to the NASA Access Help Desk at (301) 621-0134
- Telephone the NASA Access Help Desk at (301) 621-0390
- Write to:  
NASA Access Help Desk  
NASA Center for AeroSpace Information  
800 Elkridge Landing Road  
Linthicum Heights, MD 21090-2934



# **Corrosion Studies of 2195 Al-Li Alloy and 2219 Al Alloy With Differing Surface Treatments**

*M.D. Danford and M.J. Mendrek*

*Marshall Space Flight Center, Marshall Space Flight Center, Alabama*

National Aeronautics and  
Space Administration

Marshall Space Flight Center

Available from:

NASA Center for AeroSpace Information  
800 Elkridge Landing Road  
Linthicum Heights, MD 21090-2934  
(301) 621-0390

National Technical Information Service  
5285 Port Royal Road  
Springfield, VA 22161  
(703) 487-4650

## TABLE OF CONTENTS

1.	INTRODUCTION .....	1
2.	THE SCANNING REFERENCE ELECTRODE TECHNIQUE .....	2
3.	EXPERIMENTAL PROCEDURES .....	3
3.1	SRET Measurements .....	3
3.2	Corrosion Rate Measurements .....	3
4.	RESULTS AND DISCUSSION .....	5
4.1	Area Map Scans .....	5
4.1.1	Soda Blasted 2195 Al-Li .....	5
4.1.2	Conversion Coated 2195 Al-Li .....	8
4.1.3	Soda Blasted Conversion Coated 2195 Al-Li .....	8
4.1.4	Soda Blasted 2219 Al .....	11
4.1.5	Conversion Coated 2219 Al .....	12
4.1.6	Soda Blasted Conversion Coated 2219 Al .....	12
4.2	Corrosion Rate Measurements .....	15
4.2.1	2195 Al-Li .....	15
4.2.2	2219 Al .....	18
5.	CONCLUSIONS .....	23
	REFERENCES .....	24

## LIST OF FIGURES

1.	The scanning reference electrode system .....	2
2.	Uncoated 2219-T87 Al alloy after 2 hours .....	5
3.	Uncoated 2219-T87 Al alloy after 3 hours .....	6
4.	Uncoated 2195 Al-Li alloy after 2 hours .....	6
5.	Uncoated 2195 Al-Li alloy after 3 hours .....	7
6.	Soda blasted 2195 Al-Li alloy after 2 hours .....	7
7.	Soda blasted 2195 Al-Li alloy after 4 hours .....	8
8.	Conversion coated 2195 Al-Li alloy after 2 hours .....	9
9.	Conversion coated 2195 Al-Li alloy after 4 hours .....	9
10.	Soda blasted conversion coated 2195 Al-Li alloy after 2 hours .....	10
11.	Soda blasted conversion coated 2195 Al-Li alloy after 4 hours .....	10
12.	Soda blasted 2219-T87 Al alloy after 2 hours .....	11
13.	Soda blasted 2219-T87 Al alloy after 4 hours .....	12
14.	Conversion coated 2219-T87 Al alloy after 2 hours .....	13
15.	Conversion coated 2219-T87 Al alloy after 4 hours .....	13
16.	Soda blasted conversion coated 2219-T87 Al alloy after 2 hours .....	14
17.	Soda blasted conversion coated 2219-T87 Al alloy after 4 hours .....	14
18.	Corrosion pattern for bare 2195 Al .....	16
19.	Corrosion pattern for soda blasted 2195 Al .....	16
20.	Corrosion pattern for conversion coated 2195 Al .....	17
21.	Corrosion pattern for soda blasted conversion coated 2195 Al .....	17
22.	Corrosion pattern for bare 2219 Al .....	18
23.	Corrosion pattern for soda blasted 2219 Al .....	19
24.	Corrosion pattern for conversion coated 2219 Al .....	19
25.	Corrosion pattern for soda blasted conversion coated 2219 Al .....	20

## LIST OF FIGURES (Continued)

26.	Equivalent circuit model used for analysis of EIS data .....	20
27.	Corrosion pattern for aluminum oxide blasted 2219 Al .....	21
28.	Corrosion rates for primer coated samples .....	21

## TECHNICAL PAPER

### CORROSION STUDIES OF 2195 Al-Li ALLOY AND 2219 Al ALLOY WITH DIFFERING SURFACE TREATMENTS

#### 1. INTRODUCTION

The purpose of this study was to evaluate the use of sodium bicarbonate ( $\text{NaHCO}_3$ ) used in the soda blast process for preparing the surfaces of metal alloys for further possible treatment with corrosion inhibitors or paint, and to determine the corrosion protection afforded by this treatment. Electrochemical methods were used for the entire study. The water blast process using  $\text{NaHCO}_3$  as an abrasive medium is known to provide a good adhesive surface for the application of paint,<sup>1</sup> but its ability to provide corrosion protection to aluminum (Al) alloys is somewhat in question. As a result, this work concentrated on a study of the corrosion mechanisms and corrosion rates for 2219-T87 aluminum (Al) and 2195 Al-Lithium (Al-Li) alloys. Comparisons are made between the soda blast process and conversion coats, or combinations thereof, in providing corrosion protection for these alloys. Use was made of the Scanning Reference Electrode Technique (SRET), the dc Polarization Resistance Technique.<sup>2-4</sup> In addition, primer coated 2219 Al samples were evaluated using the alternating current (ac) Electrochemical Impedance Spectroscopy technique.<sup>5</sup>



## 2. THE SCANNING REFERENCE ELECTRODE TECHNIQUE (SRET)

The SRET instrument, shown in figure 1, is commercially available from EG&G Princeton Applied Research Corporation (EG&G-PARC). It has the capability to measure microgalvanic potentials close to the surface of materials, and allows in-situ examination and quantification, on a microscopic scale, of electrochemical activity as it occurs. The SRET is microprocessor controlled, and electrochemical potentials are measured by a special probe capable of translation in the x and y directions. The specimen, in the form of a cylinder, is held in a vertical position and rotated around the y axis. The scan is synchronized with a display monitor and the resultant data are shown in the form of either line scans (x direction only) or 2-dimensional area maps (x and y directions). The width of the area maps (x direction) can be set at will using the zoom-in feature of the experimental setup. The height of the area maps (y direction) is set automatically by the control software according to the proper aspect ratio. Movement of the scanning probe during data collection is in the y direction. Direct measurement of surface potentials, showing anodic and cathodic areas, at discrete positions on the sample surface, may be taken and stored for time-related studies. Because the minimum detectable signal (MDS) is of the order of  $1 \text{ mA/cm}^2$ , a potential must be applied to the sample to increase the corrosion current to at least this level, accomplished by means of a separate potentiostat (EG&G Model 273A Potentiostat/Galvanostat) coupled to the SRET system.

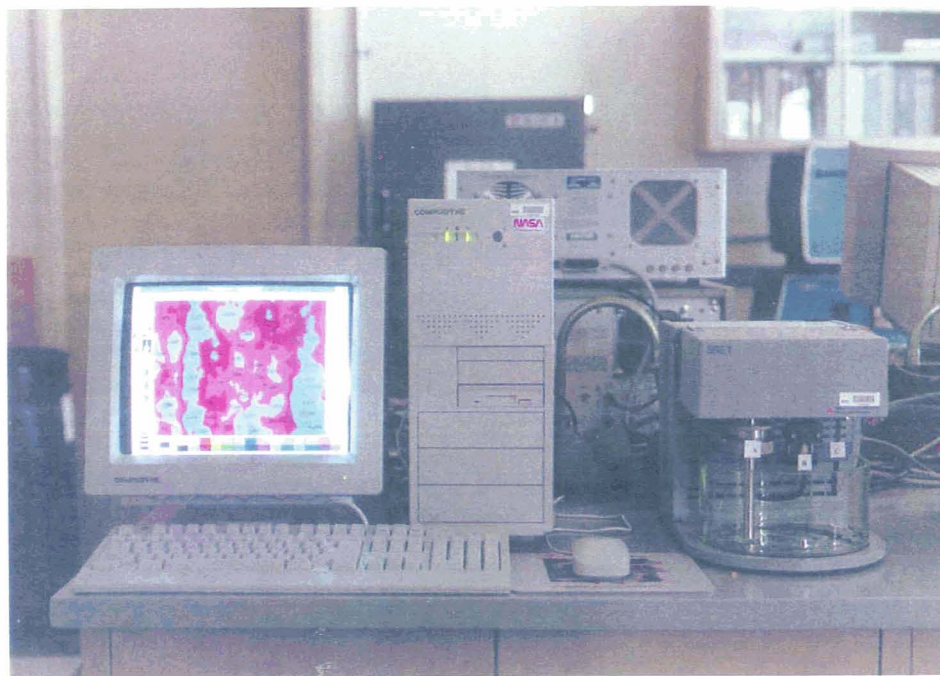


Figure 1. The scanning reference electrode system.

### 3. EXPERIMENTAL PROCEDURES

#### 3.1 SRET Measurements

SRET measurements were performed on each of four samples of the 2195 Al-Li alloy. These consisted of the bare metal, soda blasted sample, conversion coated sample and a sample with a soda blasted surface subsequently coated with a conversion coat. The process was repeated for 2219-T87 Al, making a total of eight samples measured. The samples consisted of cylindrical metal rods 10.2 cm (4 in.) long having a diameter of approximately 1.27 cm (0.5 in.). For each experiment, the test specimen was mounted in the collet of the SRET system and the probe, counter electrode and reference electrode were placed in their proper positions in the machine. The probe was then driven to a position such that the point was approximately 0.5 to 1.0 mm from the metal cylinder, and the entire assembly was immersed in a corrosive medium consisting of a 3.5-percent sodium chloride solution. About a 5.1-cm (2-in.) length of the metal sample rod was thus exposed to the corrosive medium. A potential noble (more positive than) to the normal corrosion potential ( $E_{\text{corr}}$ ) was then applied to the metal sample rod. This applied potential was approximately the same for all samples (about 200 mV) and resulted in a current well above the MDS level. During data collection the samples were rotated at 100 revolutions per minute (rpm). All maps had a width of 3.0 cm (x direction) and a height of 2.25 cm (y direction). Three area maps were collected for each sample, with a 2-hour delay between each. After data collection was completed, each map was displayed on the computer screen and the proper palette (color scheme) for display of map features (potentials for anodic and cathodic features) was obtained using software developed for this purpose. Potentials of the positive cathodic features and the negative anodic features in millivolts (mV) were measured with the same software, and were typed on the maps in their appropriate positions using other software.

#### 3.2 Corrosion Rate Measurements

Data for the determination of the normal corrosion rates (at zero potential with respect to  $E_{\text{corr}}$ ) for each of the samples exposed to a 3.5-percent sodium chloride solution, a highly corrosive medium, were obtained using the dc Polarization Resistance technique, with data collected using the EG&G instrumentation and software. The potential applied to the specimen during the scan was varied from -20 mV to +20 mV on either side of the corrosion potential  $E_{\text{corr}}$ , and the data points (current and potential) were recorded in 1/4 mV increments. The corrosion current at  $E_{\text{corr}}$  cannot be observed directly, but must be calculated. In this case, the data were analyzed using the computer program POLCURR,<sup>6</sup> a non-linear least squares program which fits the entire polarization resistance curve. Flat plates for each of the samples, the same materials and coatings as those used for the SRET measurements, were clamped in separate flat cells manufactured by EG&G-PARC. An area of 1 cm<sup>2</sup> was continuously exposed to the 3.5-percent sodium chloride solution. Corrosion currents for each were measured over a period of 2 weeks using the PR method, with data for each sample being collected on alternate days. Each measured result is the average of three separate determinations. The average time for each point was about 1 hour using this method. Silver/silver chloride reference electrodes were used in all cases.

Three plates of 2219 Al alloy, each coated with 15.5 microns of Deft #44-GN-7 primer, were also studied using the EIS technique. Preliminary treatment with an Alodine conversion coat, soda blast and  $\text{Al}_2\text{O}_3$  blast, one treatment to each of the three plates, was provided, after which each plate was coated with the Deft primer.

## 4. RESULTS AND DISCUSSION

### 4.1 Area Map Scans

Because area map scans of the bare metal corrosion were made at a potential of 100 mV, whereas the map scans of the coated metals were made at a potential of 200 mV, it is difficult to compare the corrosion mechanisms of the bare metals with those for the metals which have had surface treatments. However, the applied potential for all of the surface-treated metals is the same, so that comparisons can be more easily made. All map scans were obtained using the SRET system.

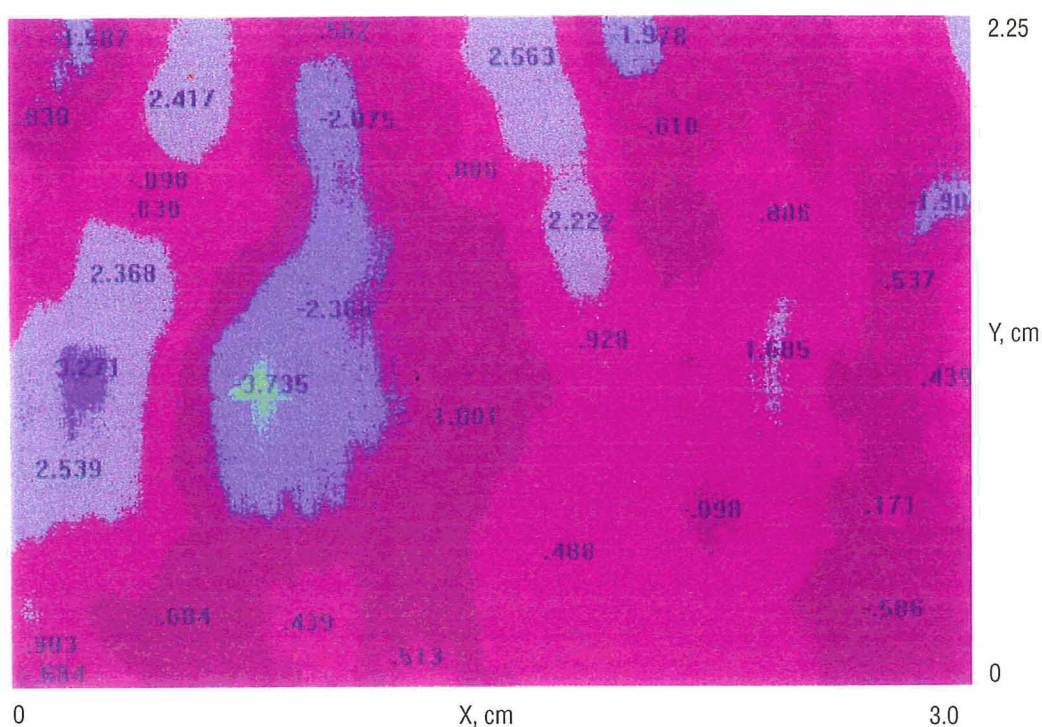


Figure 2. Uncoated 2219-T87 Al alloy after 2 hours.

#### 4.1.1 Soda Blasted 2195 Al-Li

Maps for soda blasted 2195 Al-Li are shown in figures 6 and 7, taken after 2 and 4 hours of exposure. The rate of corrosion current increase is becoming smaller between the 2- and 4-hour exposure times. The number of anodic spots is less than that for the bare metal, shown in figures 4 and 5, and these spots are a little weaker than those for the bare metal. Thus, the corrosion mechanism appears to be less localized than that for the bare metal. The number of anodic spots and the strength of these spots increases between the 2- and 4-hour times, which does not indicate a pronounced tendency toward passivation.



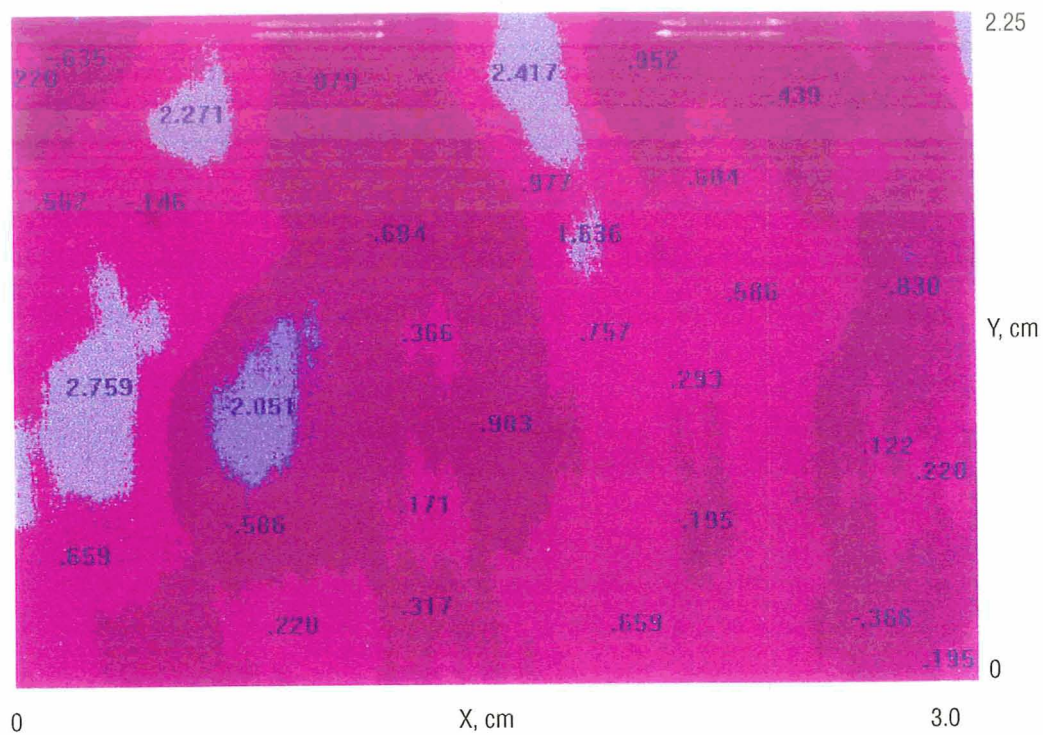


Figure 3. Uncoated 2219-T87 Al alloy after 3 hours.

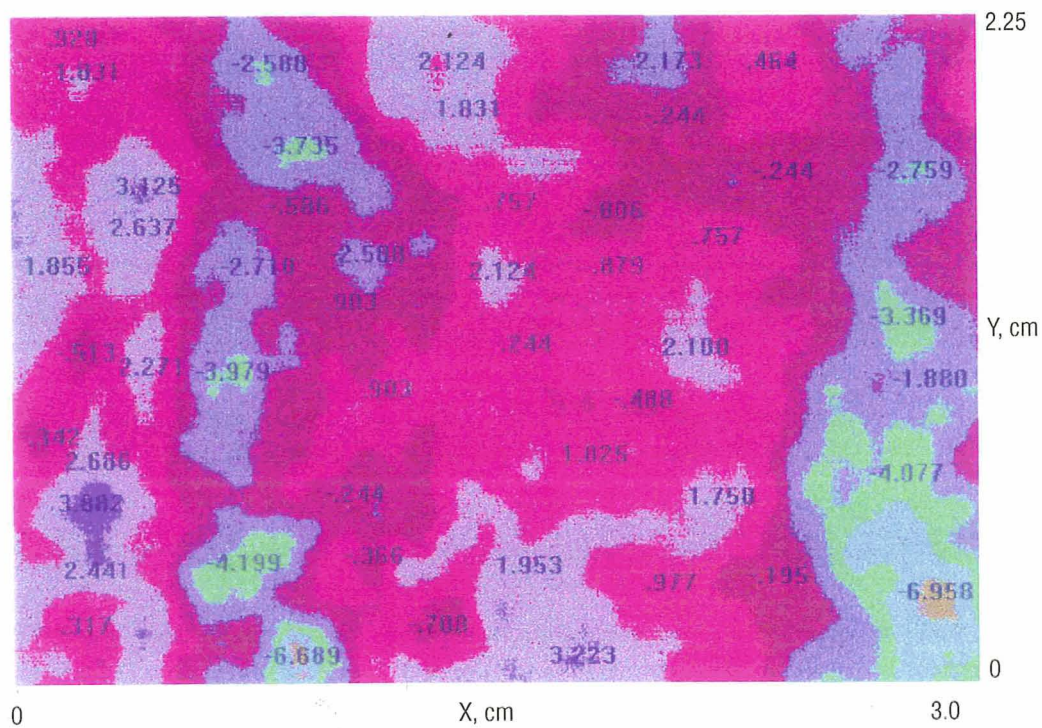


Figure 4. Uncoated 2195 Al-Li alloy after 2 hours.



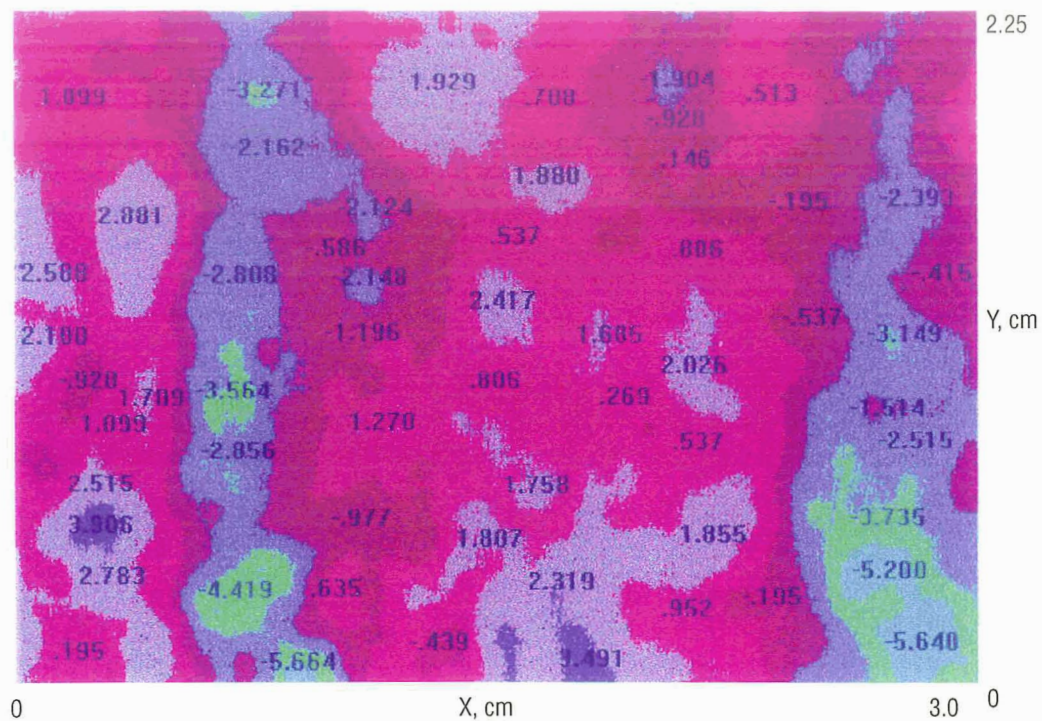


Figure 5. Uncoated 2195 Al-Li alloy after 3 hours.

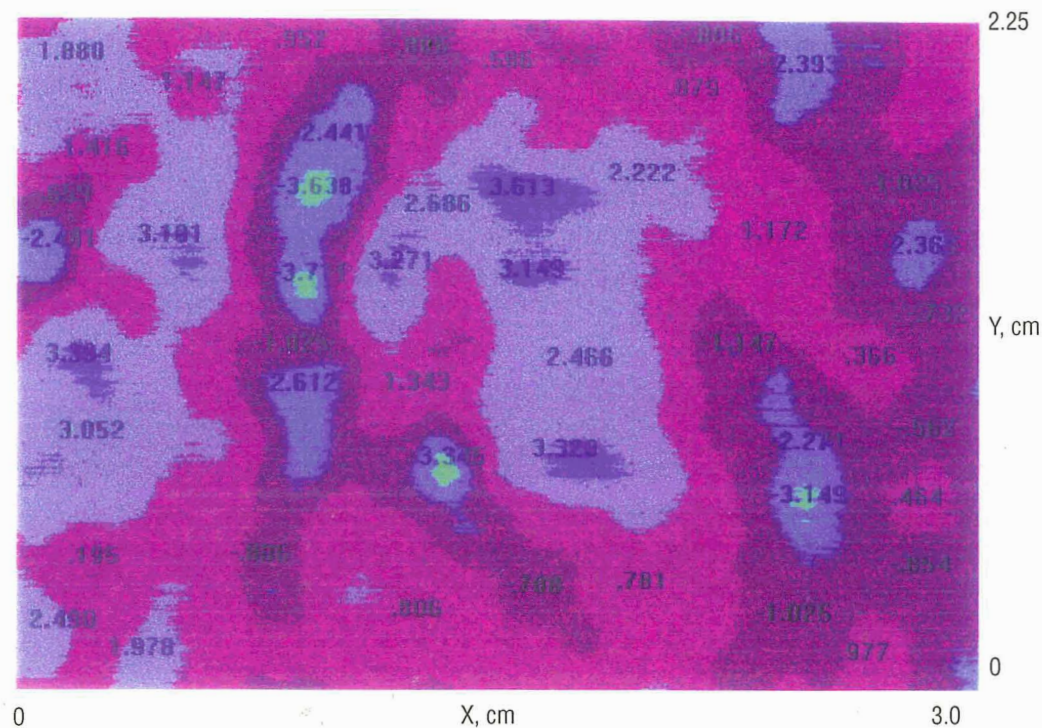


Figure 6. Soda blasted 2195 Al-Li alloy after 2 hours.







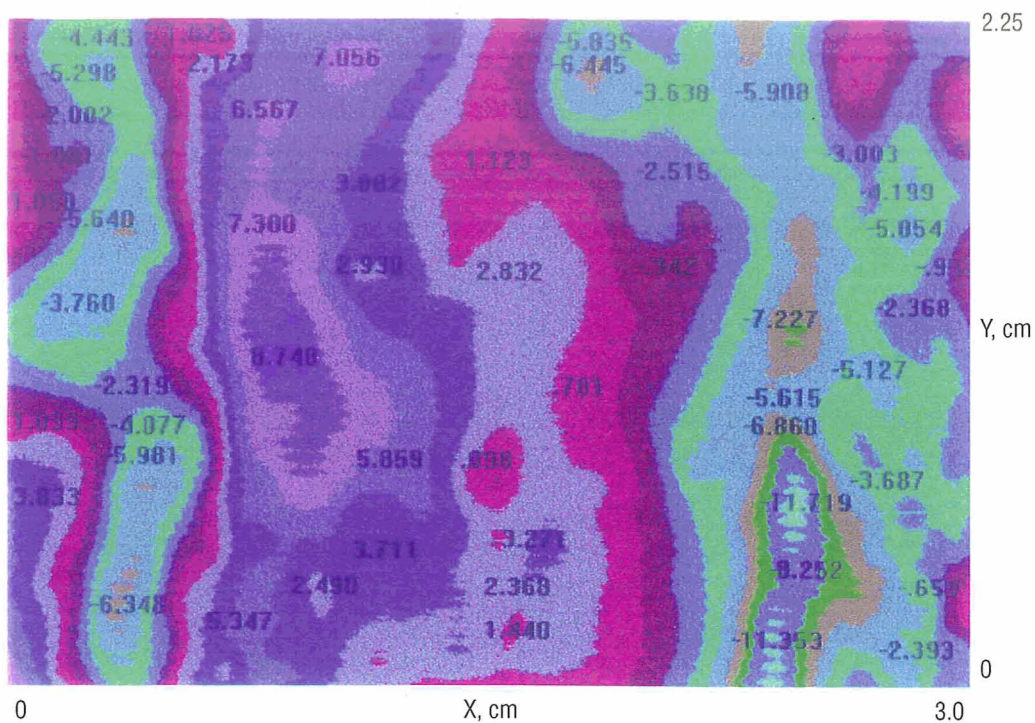


Figure 8. Conversion coated 2195 Al-Li alloy after 2 hours.

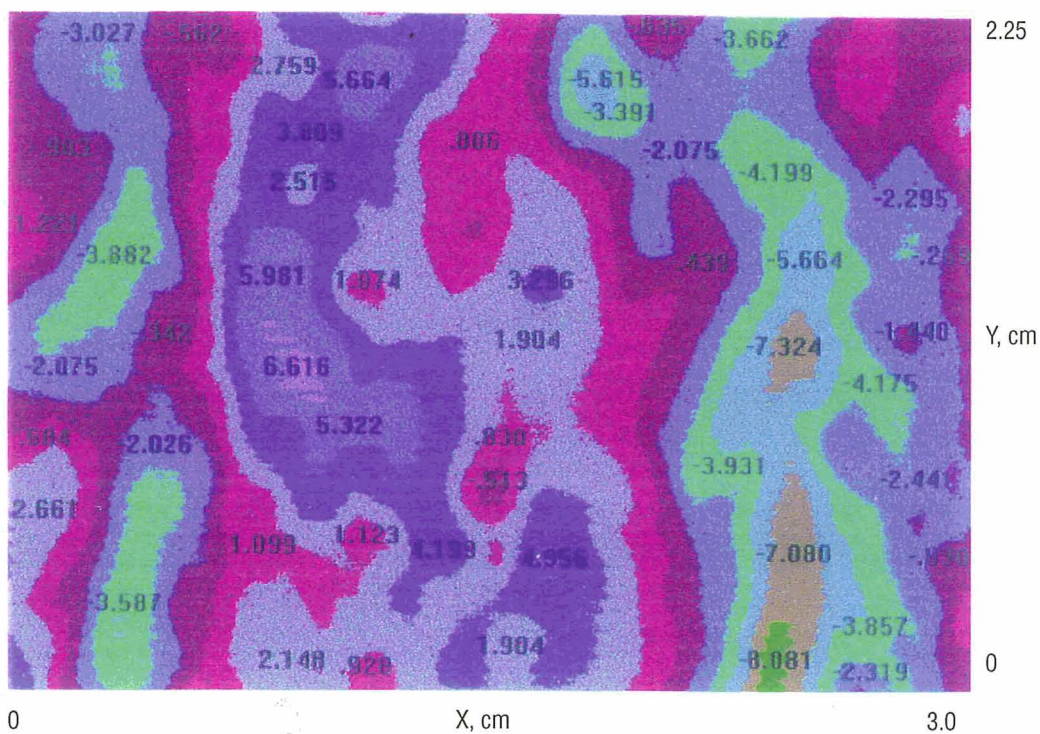


Figure 9. Conversion coated 2195 Al-Li alloy after 4 hours.



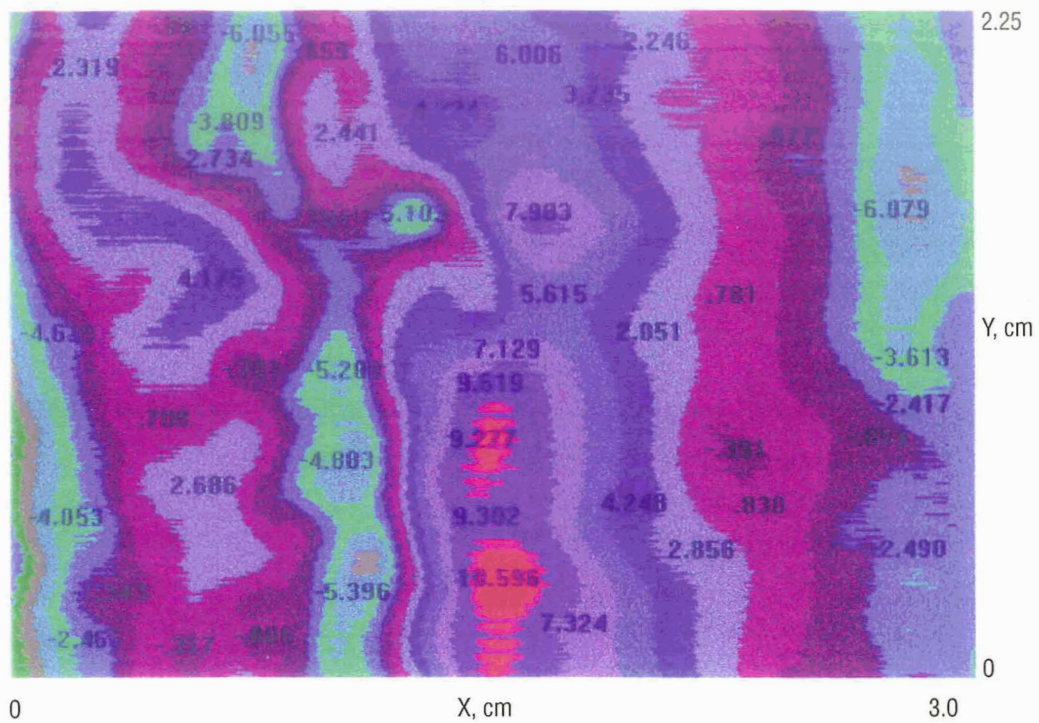


Figure 10. Soda blasted conversion coated 2195 Al-Li Alloy after 2 hours.

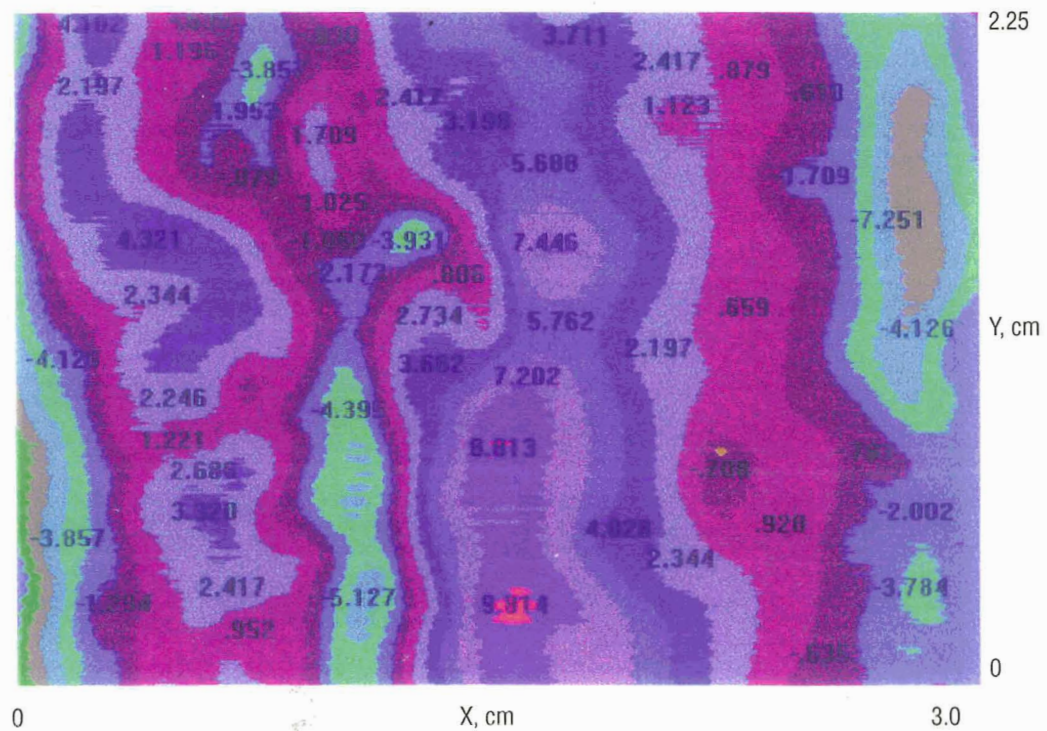


Figure 11. Soda blasted conversion coated 2195 Al-Li alloy after 4 hours.

#### 4.1.4 Soda Blasted 2219 Al

Maps for soda blasted 2219 Al after 2 and 4 hours of exposure are shown in figures 12 and 13 respectively. The features in the corrosion map at the 2-hour point are much more localized and stronger than those for the bare metal. The rate of increase in the corrosion current becomes very small between the 2- and 4-hour maps. The number of anodic spots remains about the same in the 4-hour map as in the 2-hour map, but the strengths of these spots are generally becoming much lower. The corrosion pattern is less highly localized than in the soda blasted 2195 Al-Li, shown in figure 7. Thus, the 2219 Al is less subject to pitting than the 2195 Al-Li. The total overall current for this coating is about the same as that for the soda blasted 2195 Al-Li in figures 6 and 7.

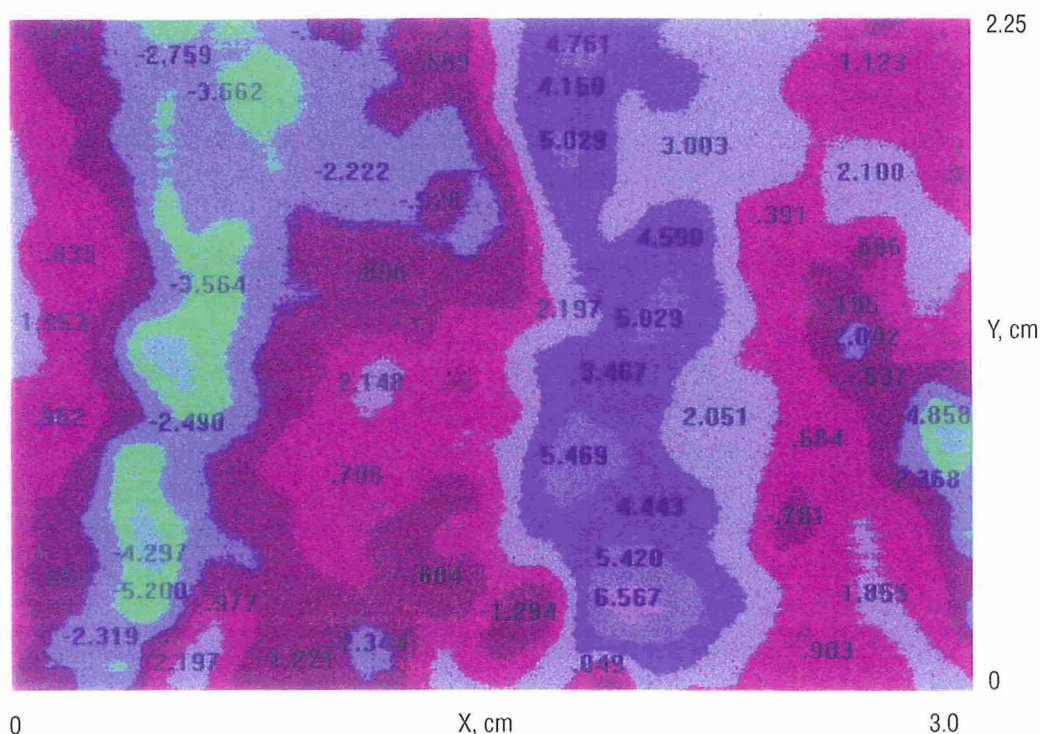


Figure 12. Soda blasted 2219-T87 Al alloy after 2 hours.



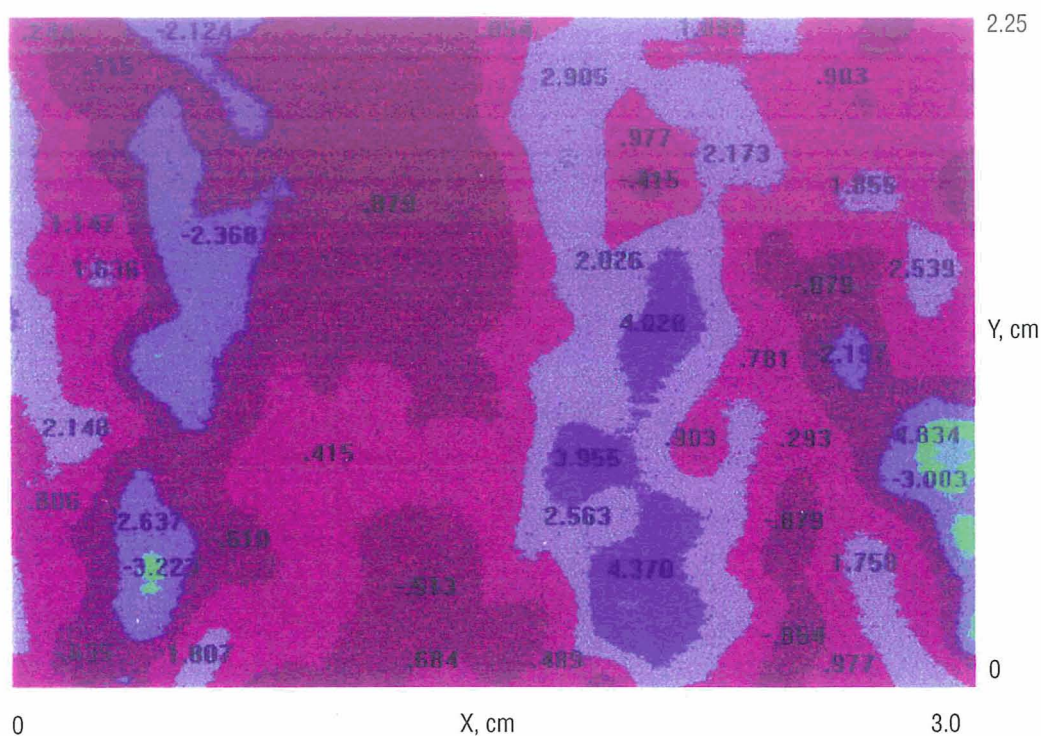


Figure 13. Soda blasted 2219-T87 Al alloy after 4 hours.

#### 4.1.5 Conversion Coated 2219 Al

Maps for this sample are shown in figures 14 and 15. Again, this alloy shows a very highly localized corrosion mechanism, with the number of anodic spots about the same as that for the 2195 Al-Li alloy in figures 10 and 11. The strengths of the anodic spots are even greater than those for the 2195 Al-Li alloy at the 2-hour point. The rate of total corrosion current is not as great as in the case of the 2195 Al-Li alloy during the first two hours, and this current decreases only a small amount between 2 and 4 hours. Contrary to the behavior of the 2195 Al-Li alloy, the number of anodic spots actually increases with time, with the strengths of these spots even greater in many cases. The total overall current for this case is about the same as that for the conversion coated 2195 Al-Li.

#### 4.1.6 Soda Blasted Conversion Coated 2219 Al

Maps for this case are shown in figures 16 and 17. The overall corrosion picture for this alloy is much less highly localized than that for the 2195 Al-Li alloy in figures 10 and 11. In this case, the number of strong anodic spots is much lower than that for the 2195 Al-Li alloy. The rate of total corrosion current decrease between the 2- and 4-hour points is a little less than that for the similarly coated 2195 Al-Li alloy, with the strengths of the anodic spots also being lower. Thus, some passivation of these spots is occurring and the number of spots is becoming less. The total corrosion current in this case is comparable to that for the soda blasted-conversion coated 2195 Al-Li alloy.

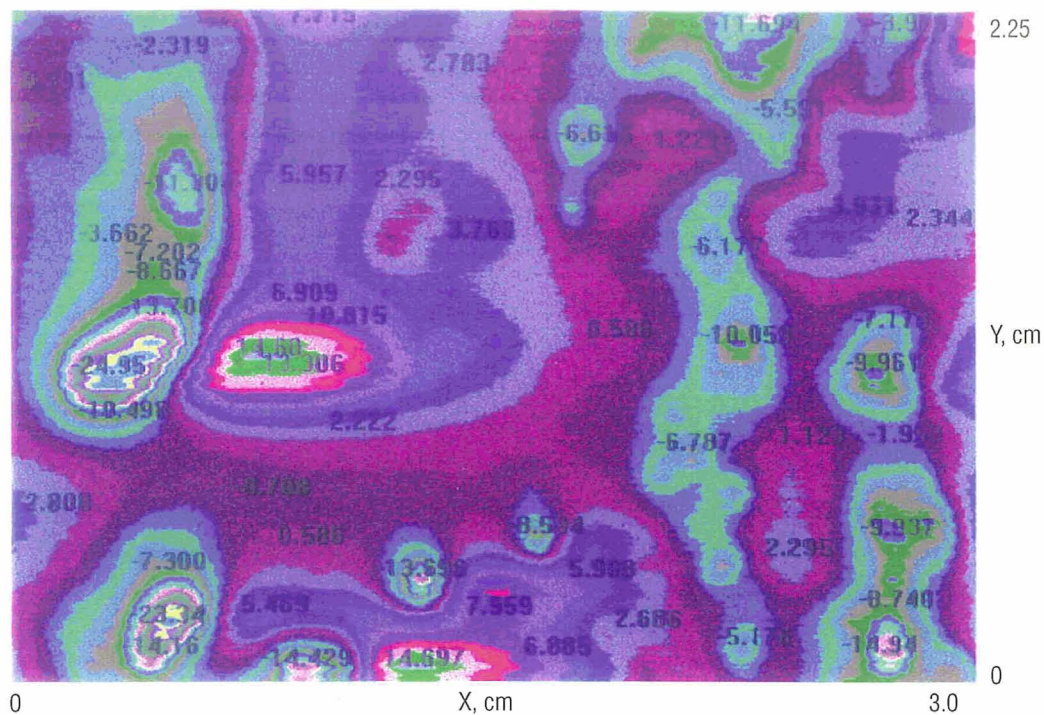


Figure 14. Conversion coated 2219-T87 Al alloy after 2 hours.

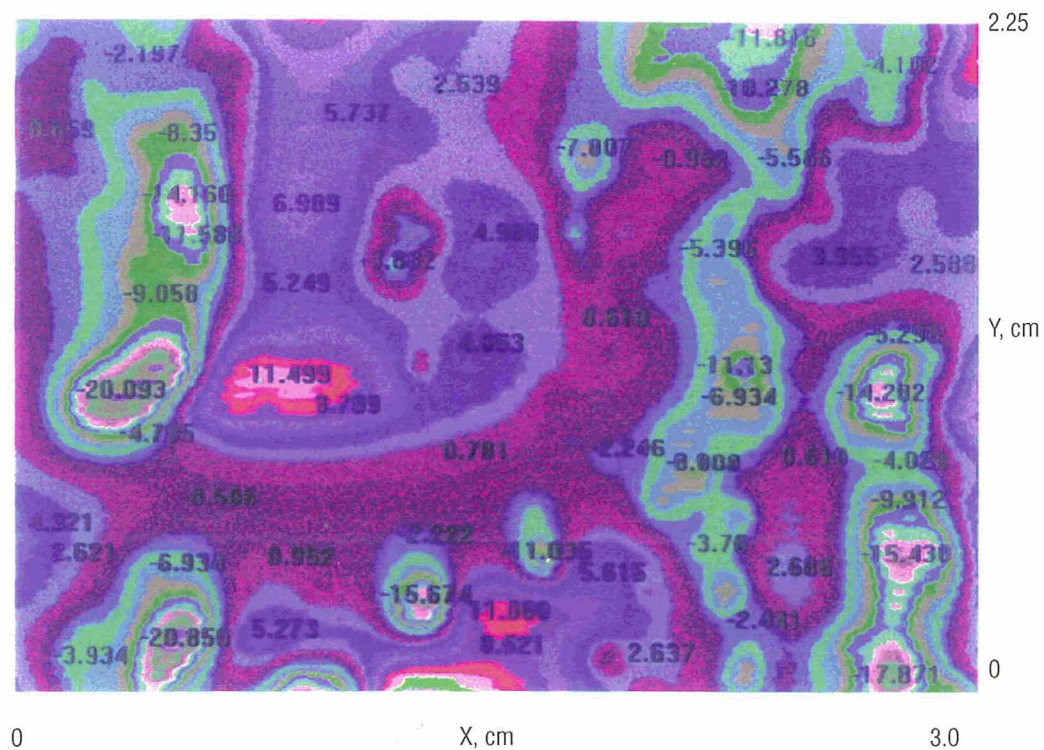


Figure 15. Conversion coated 2219T-87 Al alloy after 4 hours.



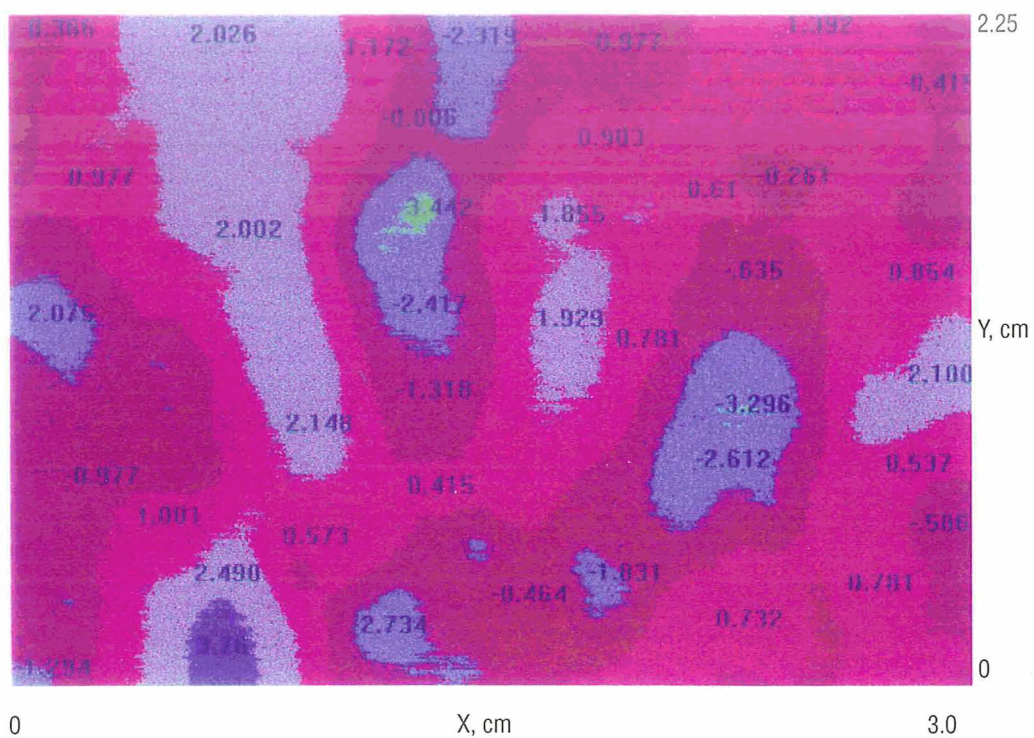


Figure 16. Soda blasted conversion coated 2219-T87 Al alloy after 2 hours.

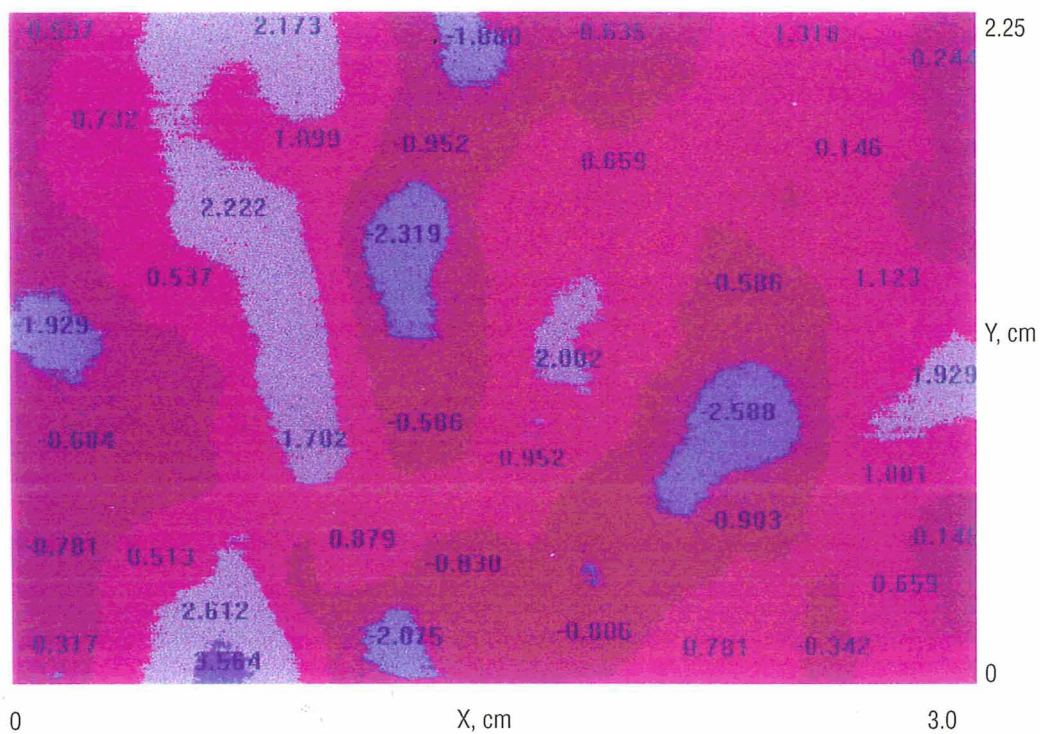


Figure 17. Soda blasted conversion coated 2219-T87 Al alloy after 4 hours.

## 4.2 Corrosion Rate Measurements

### 4.2.1 2195 Al-Li

Mean corrosion rates, averaged over the 14 day observation period, and their trends, as calculated using the linear regression technique, are listed in table 1. These are in general agreement with those which would be predicted from the SRET measurements. The average corrosion rates for the bare and soda blasted 2195 Al-Li samples are practically the same, indicating that the soda blast process alone does not alter the overall corrosion rate. However, in all cases, the corrosion mechanisms are all altered according to the SRET results, usually indicating a pronounced tendency toward a more highly localized mechanism in all cases, which would lead to a greater tendency to pit formation for 2195 Al-Li. The lowest corrosion rate in this case is that for the conversion coated soda blasted sample, showing that the effect of the double treatment is highly beneficial in lowering the overall corrosion rate in this case. Corrosion rate vs. time curves are shown in figures 18 through 21 for the 2195 Al-Li samples. The mean slopes are mixed, the curves for the bare 2195 Al-Li and the conversion coated 2195 Al-Li samples being negative, while those for the other two cases are positive.

Table 1. Mean corrosion rates and slopes for coated 2219 Al and 2195 Al.

Coating	2195 Al-Li		2219 Al	
	Corrosion rate, mils/yr	Slope, mils/yr/day	Corrosion rate, mils/yr	Slope, mils/yr/day
Bare	0.0666	$-2.7 \times 10^{-3}$	0.3904	$-1.71 \times 10^{-2}$
Soda blast	0.0639	$1.0 \times 10^{-4}$	0.3938	$-1.31 \times 10^{-2}$
Conversion coat	0.0787	$-6.0 \times 10^{-4}$	0.0132	$-1.110 \times 10^{-3}$
Conversion coat, Soda blast	0.0232	$4.2 \times 10^{-3}$	0.0877	$1.400 \times 10^{-3}$
Al <sub>2</sub> O <sub>3</sub> blast			0.1847	$-4.0 \times 10^{-4}$

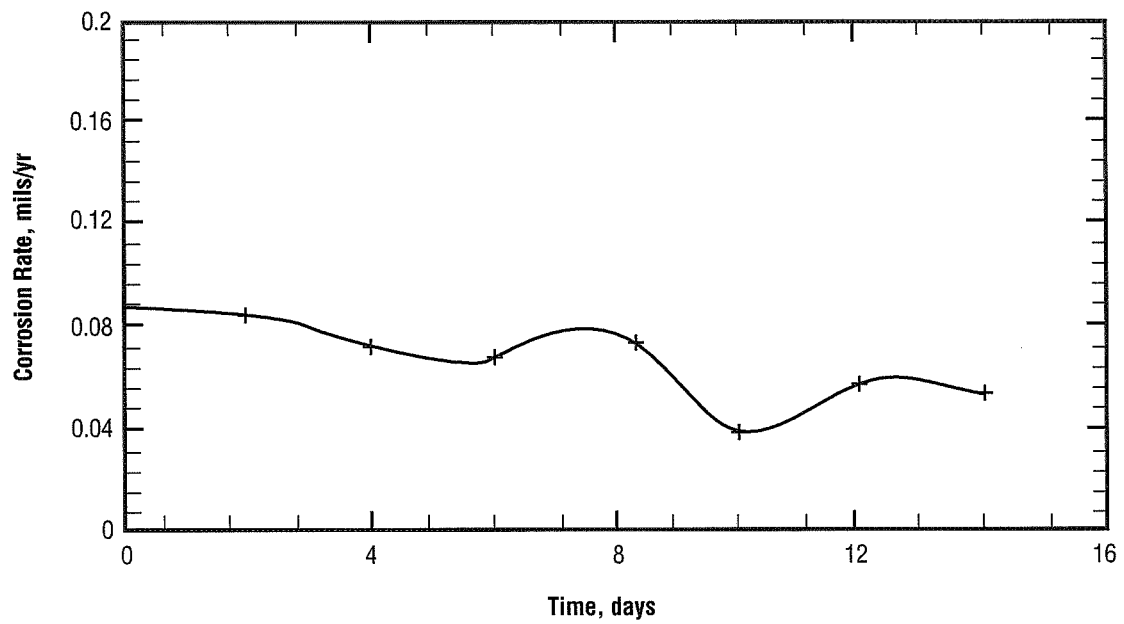


Figure 18. Corrosion pattern for bare 2195 Al.

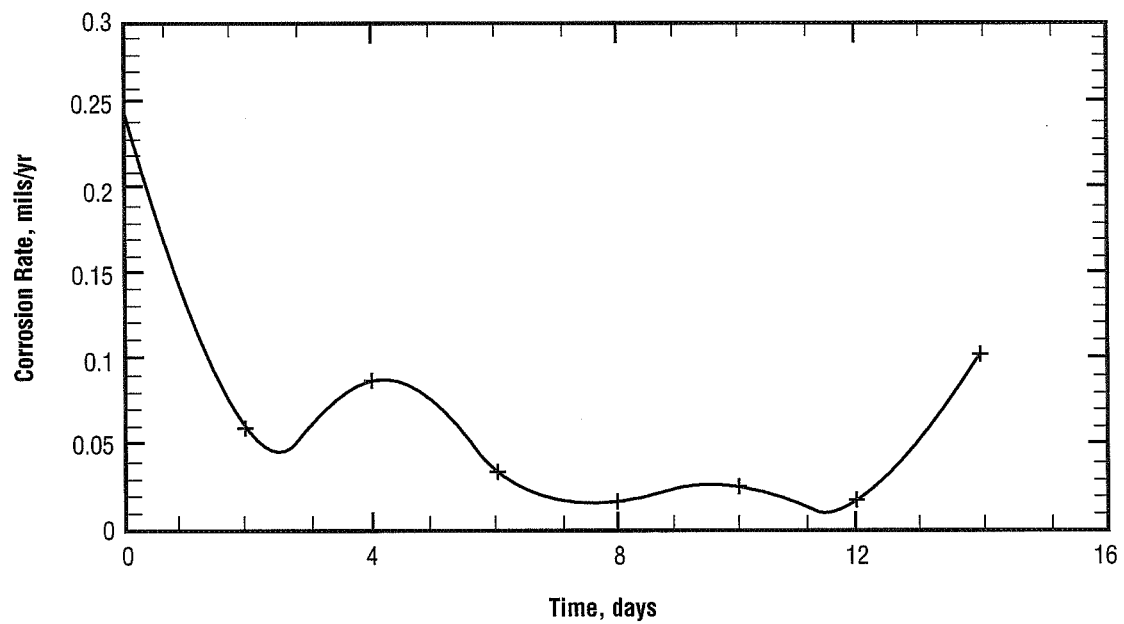


Figure 19. Corrosion pattern for soda blasted 2195 Al.

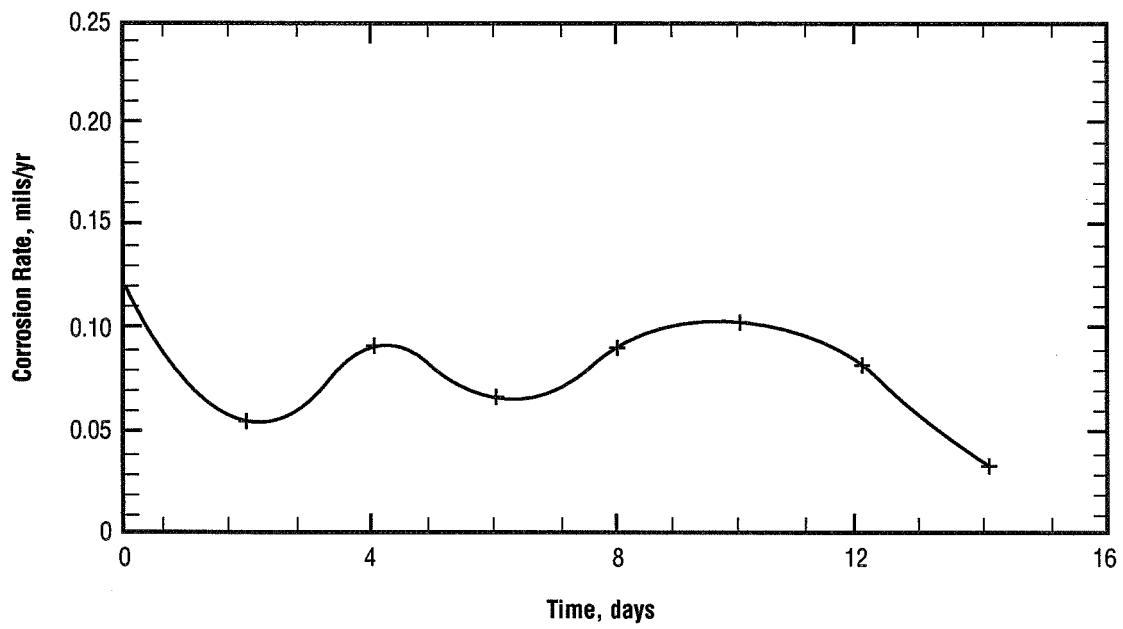


Figure 20. Corrosion pattern for conversion coated 2195 Al.

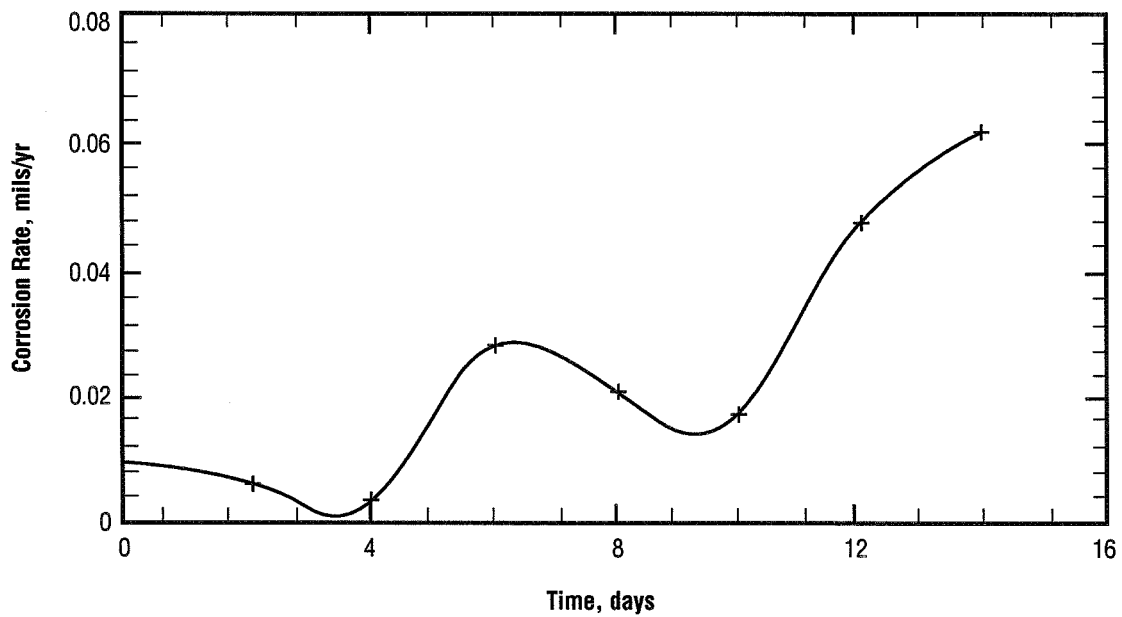


Figure 21. Corrosion pattern for soda blasted conversion coated 2195 Al.



#### 4.2.2 2219 Al

Corrosion rates and mean slopes are also listed in table 1 for this case. In most cases, the average corrosion rates are higher than those for the 2195 Al-Li, the exception being in the case of the conversion coated samples. The primary reason for the higher observed corrosion rates is that the corrosion rates are much higher on the first day of measurement than in the case of the 2195 Al-Li alloy. Again, the corrosion rate is not affected by use of the soda blast process, the corrosion rates for bare and soda blasted 2219 Al being practically the same. The trends are generally not in good accord with those from the SRET measurements, contrary to the results obtained in the case of 2195 Al-Li. The mean slopes are all negative, with the exception of the soda blasted conversion coated 2219 Al alloy. Corrosion rate vs. time curves are shown in figures 22 through 25. A sample with an  $\text{Al}_2\text{O}_3$  blast treatment indicated a significant improvement in the corrosion rate over that with the soda blast process, as shown in table 1. The equivalent circuit model used for the interpretation of EIS data is shown in figure 26. Values for each of the circuit components in figure 26 were treated as parameters in the nonlinear ORGLS<sup>7</sup> least-squares program, which automatically adjusted these parameters to obtain a best fit to the observed Bode magnitude data (log impedance versus  $\log \omega (\omega = 2\pi \times \text{frequency})$ ). Good estimates for the corrosion rates were obtained from the EIS data using the Stern-Geary equation for charge transfer control. Tafel constants ( $b_a$  and  $b_c$ ) were assumed to be 50 mV each. Corrosion rates were determined from the  $I_{\text{corr}}$  values by methods described previously.<sup>8</sup>

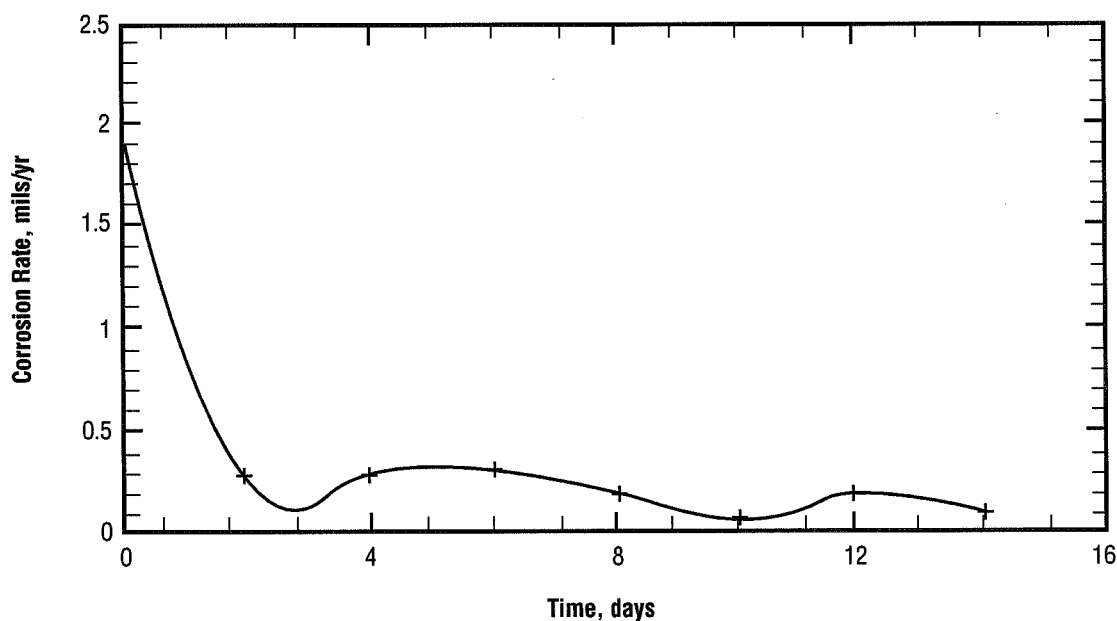


Figure 22. Corrosion pattern for bare 2219 Al.

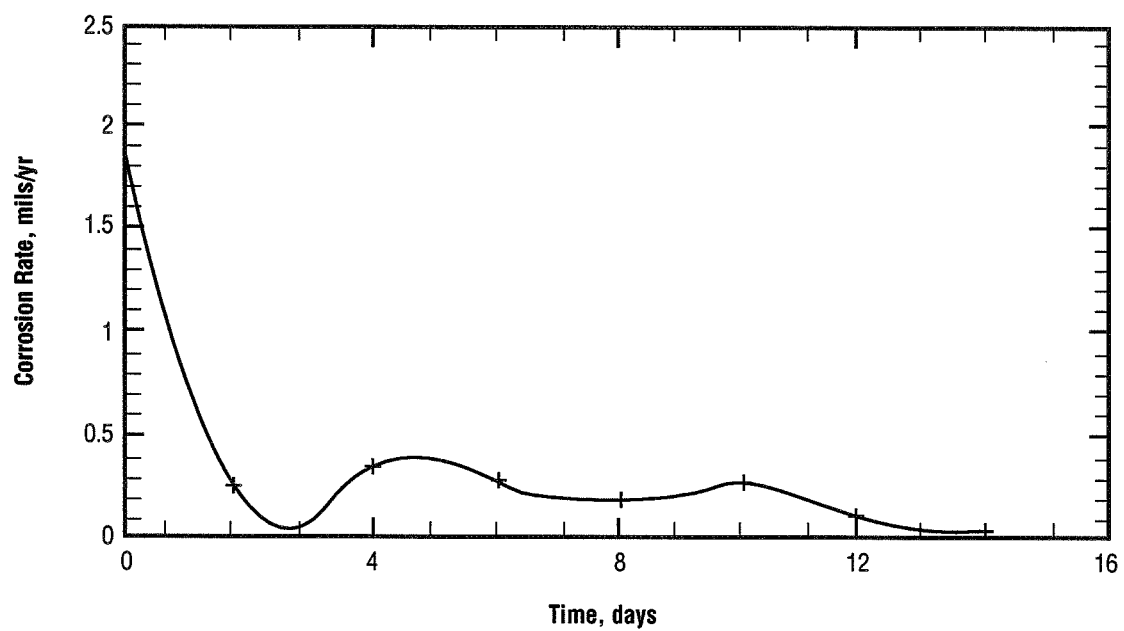


Figure 23. Corrosion pattern for soda blasted 2219 Al.

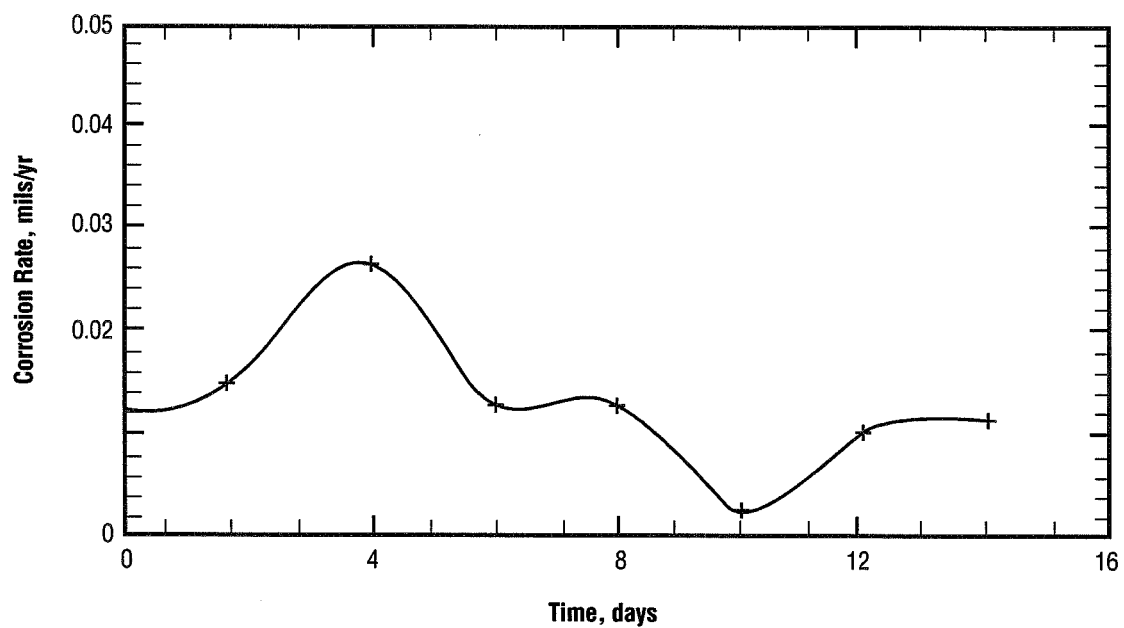


Figure 24. Corrosion pattern for conversion coated 2219 Al.

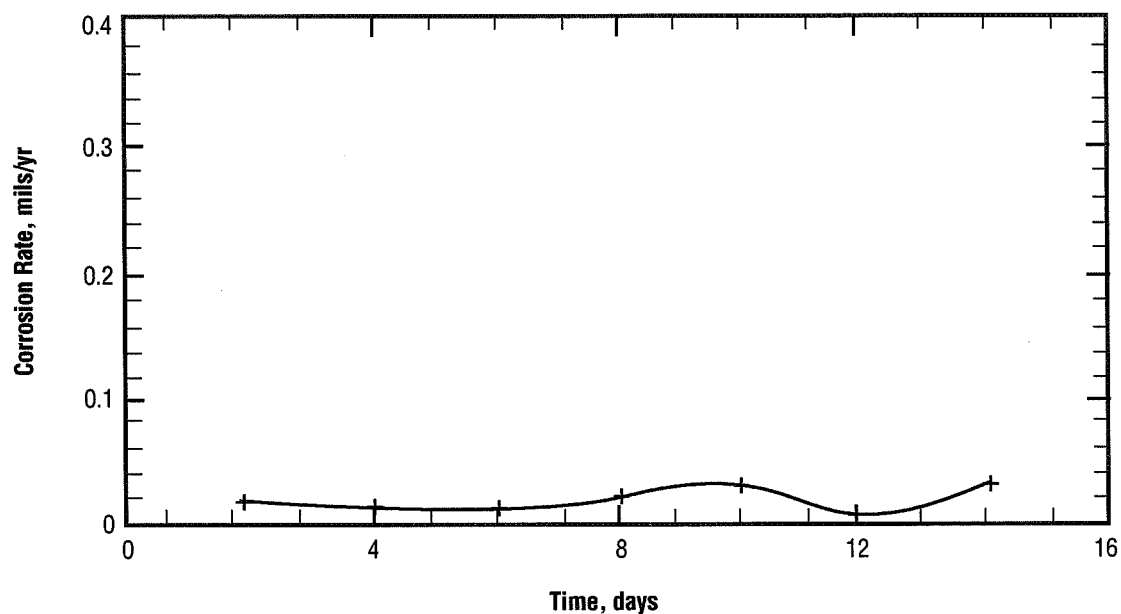


Figure 25. Corrosion pattern for soda blasted conversion coated 2219 Al.

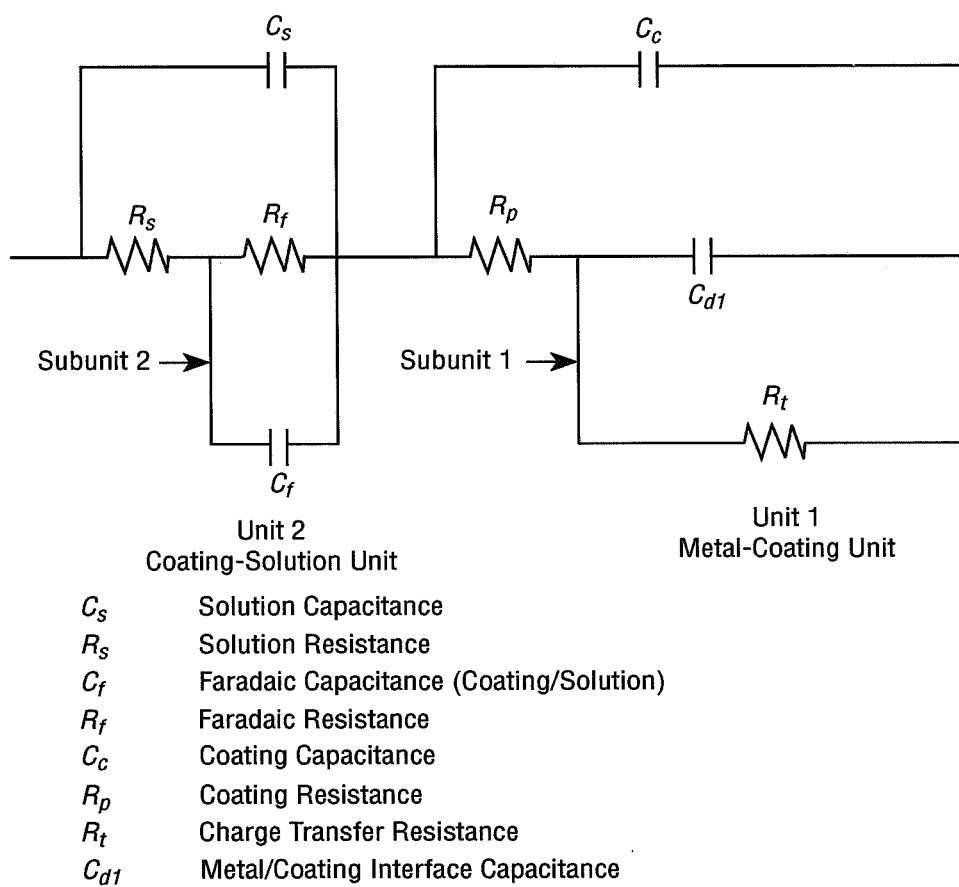


Figure 26. Equivalent circuit model used for analysis of EIS data.

A corrosion rate-time curve for  $\text{Al}_2\text{O}_3$  blasted 2219 Al is shown in figure 27. Curves are shown in figure 28 for  $\text{Al}_2\text{O}_3$  blasted, Soda blasted and conversion coated 2219 Al coated with primer, obtained using the EIS method. The soda blasted case is the worst, with the conversion coated case the best. The  $\text{Al}_2\text{O}_3$  blasted case is intermediate, reaching the level of the conversion coated case after 2 weeks. Mean corrosion rates and slopes are summarized in table 2 for the primer coated samples.

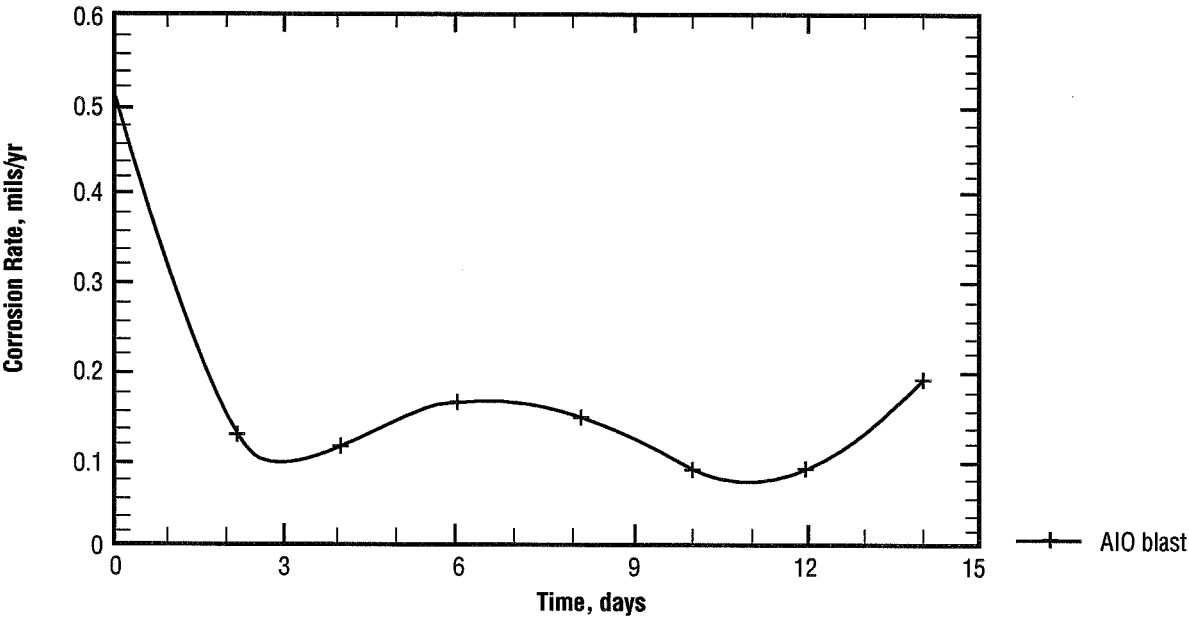


Figure 27. Corrosion pattern for aluminum oxide blasted 2219 Al.

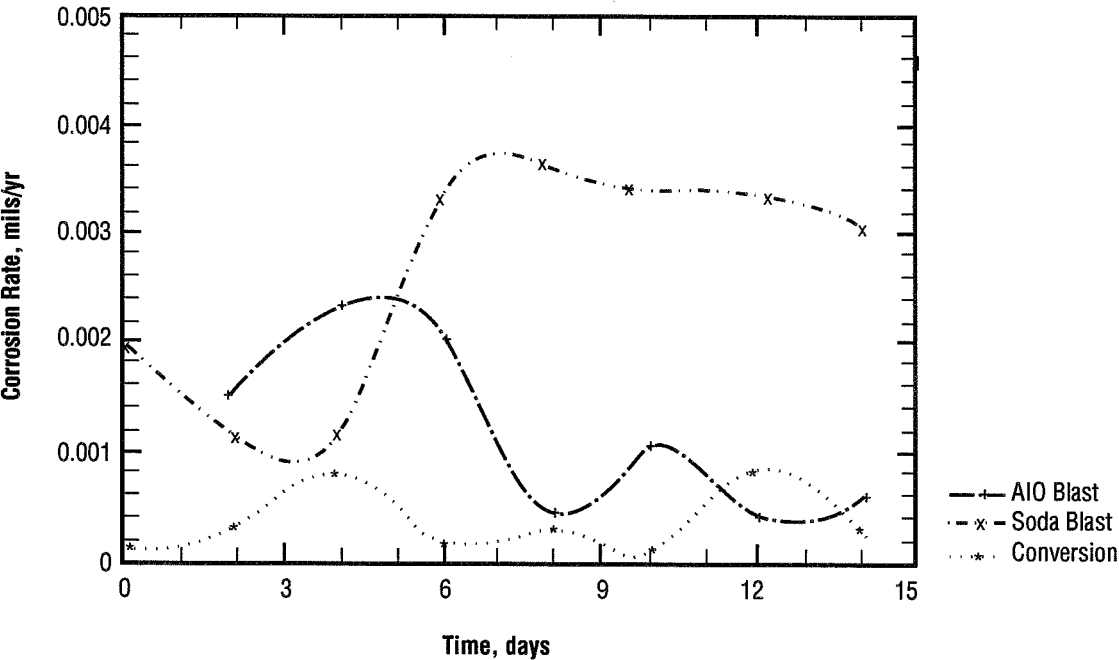


Figure 28. Corrosion rates for primer coated samples.

Table 2. Mean corrosion rates and slopes for primer coated samples.

2219 Al		
Preliminary treatment	Corrosion rate, mils/year	Slope, mils/yr/day
Soda Blast	0.002618	+0.0002
Al <sub>2</sub> O <sub>3</sub>	0.001880	-0.00010
Conversion Coat	0.0003456	-0.00004

## 5. CONCLUSIONS

For samples not treated with primer, SRET measurements indicate a tendency toward more highly localized corrosion mechanisms than those indicated by measurements of the bare metals. This would result in a more pronounced tendency toward pitting, although the overall corrosion rates are not necessarily affected. Corrosion rates observed for the 2195 Al-Li alloy are in general agreement with trends which were observed in the SRET studies, but trends for the 2219 Al alloy are in most cases not in good agreement. The measurements indicate that the soda blast process does not significantly affect the corrosion rates in the case of both the 2195 Al-Li alloy and 2219 Al alloy. However, measurements of a 2219 alloy treated with the  $\text{Al}_2\text{O}_3$  blast process indicated a significant improvement over those provided by the soda blast process. Also, the soda blast case represents the worst corrosion protection for the samples shown in figure 28 for the primer coated samples. The conversion coated case provides the best protection, and the aluminum oxide blasted case is intermediate, approaching the level of the conversion coated case after about 10 days.

## REFERENCES

1. NASA/MSFC Internal Memorandum, EH24 (95-04), Feb. 10, 1995.
2. Stern, M., and Geary, A.L.: Journal of the Electrochemical Society, Vol. 102, p. 609, 1955.
3. Stern, M., and Geary, A.L.: Journal of the Electrochemical Society, Vol. 104, p. 56, 1957.
4. Stern, M.: Corrosion, Vol. 14, p. 440t., 1958.
5. Danford, M.D.: "Equivalent Circuit Models for AC Impedance Data Analysis," NASA Technical Memorandum 100402, June 1990.
6. Gerchakov, S.M., Udey, L.R. and Mansfeld, F.: "An Improved Method for Analysis of Polarization Resistance Data." Corrosion, vol. 37, p.696, 1981.
7. Busing, W.R., and Levy, H.A.: "A General Nonlinear Least Squares Program ORGLS," Oak Ridge National Laboratory, 1958.
8. Danford, M.D.: NASA Technical Memorandum, TM-100366, April 1989.